Optimal Paths for Landmark-Based Navigation by Differential-Drive Vehicles With Field-of-View Constraints

Sourabh Bhattacharya, Rafael Murrieta-Cid, *Member, IEEE*, and Seth Hutchinson, *Fellow, IEEE*

***Abstract*—In this paper, we consider the problem of planning optimal paths for a differential-drive robot with limited sensing, that must maintain visibility of a fixed landmark as it navigates in its environment. In particular, we assume that the robot's vision sensor has a limited field of view (FOV), and that the fixed landmark must remain within the FOV throughout the robot's motion.We first investigate the nature of extremal paths that satisfy the FOV constraint. These extremal paths saturate the camera pan angle. We then show that optimal paths are composed of straight-line segments and sections of these these extremal paths. We provide the complete characterization of the shortest paths for the system by partitioning the plane into a set of disjoint regions, such that the structure of the optimal path is invariant over the individual regions.**

***Index Terms*—Nonholonomic constraints, optimal control.**

I. Introduction

In this paper, we study the interaction of the nonholonomic and visibility constraints for a differential-drive robot (DDR) with limited sensing that maintains visibility of a stationary landmark. We first demonstrate controllability of the system, and then describe optimal paths for the system.

The derivation of optimal paths for various nonholonomic systems has been addressed by numerous researchers (a nice overview is given in [1]). Some of the seminal work on these problems was done by Dubins [2] and Reeds and Shepp (RS) [3], whose results show that shortest paths for car-like robots with bounded turning radius, and that move forward (the Dubins car) or that move forward and backward (the RS car) comprise straight-line segments and arcs of circles that saturate the steering angle.

Since that work, more recent approaches have applied Pontryagin's Maximum Principle (PMP) [4] to derive shortest paths in the plane, or to derive time-optimal paths. Sussman and Tang [5] and Boissonnat *et al.* [6] used PMP along with techniques from modern geometric control theory to rederive the earlier results of RS. Soueres and Laumond [7] then built on these results, giving a complete characterization of the shortest paths for the RS car. They derive a partition of the car's configuration space, such that the structure of the optimal path to the origin is invariant over each region in the partition. Their work essentially closes the book on the problem of planning optimal paths for the RS car in an obstacle-free environment.

In addition to basic car-like robots, optimal paths have been studied for a a number of nonholonomic systems. In [8], PMP is used to demonstrate the time-optimal paths for a mobile robot with one trailer. In [9]–[11], PMP is used to address the time-optimal problems regarding underwater vehicles. In general, the only constraints imposed on the motion of these systems are the nonholonomic constraints that derive from the robot kinematics. These methods do not typically consider the possibility of obstacles in the environment, or of sensing constraints.

In recent years, a significant amount of research has been done on the problem of planning collision-free paths for nonholonomic systems, often cars or cars with trailers. In some cases, these planners are able to exploit the optimal trajectories that apply for the case when no obstacles are present. For example, Bicchi *et al.* [12] use RS curves to build a basic path diagram, which is similar to a visibility graph, but for nonholonomic vehicles. In the special case of a disc robot whose radius is equal to its minimum turning radius, paths found by this planner are optimal, though the planner is not complete, and the optimality results no longer hold for nondisc robots. Laumond *et al.* [13] present a two-stage planner, in which the first stage constructs a collision-free path that ignores the nonholonomic constraints, and the second stage recursively subdivides that path, replacing sections by optimal RS curves. In [14], the method presented in [13] is extended to the case of a car with trailer. More recently, Isler *et al.* have used the result of Dubins to address pursuit-evasion problems [15]. The success of these approaches attests to the value of studying optimal paths for nonholonomic vehicles.

DDRs comprise a special class of nonholonomic systems. Such robots have two wheels that are independently actuated (see Fig. 1), which allows them to turn in place. A number of researchers have studied the problem of deriving time-optimal paths for such robots. Reister and Pin [16] and Renaud and Fourquet [17] use a combination of analytical and numerical techniques to study the time-optimal trajectories for DDRs with independent bounds on the accelerations of the wheel. Balkcom and Mason [18] present the analytical time-optimal trajectories

Manuscript received December 27, 2005, revised August 9, 2006. This paper was recommended for publication by Associate Editor W. F. Chung and Editor K. Lynch upon evaluation of the reviewers' comments. This work was supported in part by the National Science Foundation under Awards CCR-0085917 and IIS-0083275. This paper was presented in part at the IEEE International Conference on Robotics and Automation, Orlando, FL, May 2006, and in part at the IEEE International Conference on Intelligent Robots and Systems, Sendai, Japan, 2004.

S. Bhattacharya and S. Hutchinson are with the Beckman Institute of Advanced Science and Technology, University of Illinois, Urbana, IL 61801 USA (e-mail: sbhattac@uiuc.edu; seth@uiuc.edu).

R. Murrieta-Cid is with the Center for Mathematical Research (CIMAT), A.P. 402, Guanajuato Gto., C.P. 36000, Mexico.

Color version of Fig. 9 is available online at http://ieeexplore.org.

Digital Object Identifier 10.1109/TRO.2006.886841

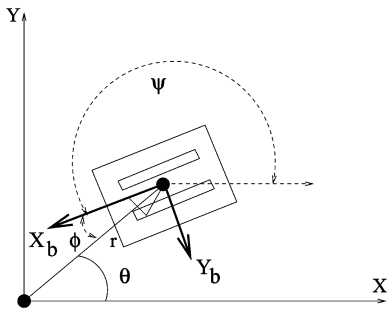

Fig. 1. Coordinate frame assignments for a DDR with camera.

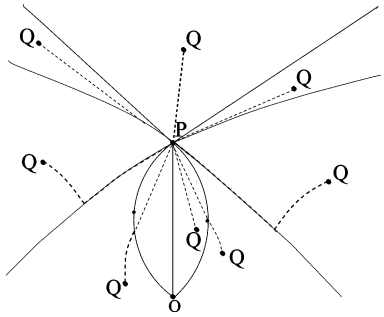

Fig. 2. Workspace partition according to nature of shortest paths.

assuming bounds on the velocities (rather than accelerations) of the wheels. In [19], they use PMP to give an elegant description of the extremal trajectories for a DDR. Further analysis leads to time-optimal trajectories between any two configurations, using the methodology of Sussman and Tang [5] and Laumond [1]. In [20], PMP is used to obtain the extremal trajectories for minimizing the amount of wheel rotation for a DDR.

In this paper, we consider the problem of planning shortest paths for DDRs whose motion is further constrained by sensing considerations. In particular, we consider the case when the robot must maintain visibility of a fixed landmark using a body-mounted camera with a limited field of view (FOV). Kantor and Rizzi [21] have considered a similar problem from a control-theory perspective. They have proposed a framework for the construction of globally convergent, purely feedback-based controllers for such a system, using the idea of variable constraint control [22], [23]. In their approach, the DDR traces a trajectory that maintains visibility of the fixed landmark while converging to the goal configuration. The resulting paths are similar to the curves we show in Section III to demonstrate controllability, but our shortest paths (developed in Sections IV–VI) can be quite different from theirs.

Our primary result is that the shortest paths for this system consist of curve segments that are either straight-line segments or that saturate the sensor viewing angle. Fig. 2 shows several examples in which the initial position is the point P and several distinct goals are denoted by Q. The fixed landmark is located at the point O. In the figure, the solid lines partition the workspace into different regions such that for each region, the shortest paths from P to any point in the region share the same structure. Example shortest paths for each region are indicated by dotted lines.

Our results are, in some ways, analogous to the earlier results of Dubins, Reeds and Shepp, and Balkcom and Mason. For each of their problems, optimal paths comprise straight-line segments and curve segments where the steering angle input is saturated (the minimum path-curvature constraint of Dubins and Reeds and Shepp giving arcs of circles, and the turn-in-place motion of Balkcom and Mason giving rotation about a point). In our case, shortest paths consist of straight-line segments and curve segments in which the pan angle of the camera is saturated. In our case, these input-saturating motions are exponential spirals.

The remainder of the paper is organized as follows. In Section II, we give the mathematical definition of the system, including the constraints imposed by the limited FOV of the camera. In Section III, we show controllability of the resulting system. In Sections IV–VI, we develop properties of shortest paths, use these properties to define a language for shortest paths, and then show shortest paths that can be constructed. Finally, in Section VII, we draw conclusions and speculate about future avenues of research.

II. Problem Definition

We make the usual assignment of body-attached frame to the robot, with origin at the midpoint between the two wheels, y-axis parallel to the axle, and the x-axis pointing forward, parallel to the heading of the robot. The configuration of the robot can be represented by (x, y, ψ), in which ψ is the angle from the world x-axis to the robot's x-axis.

The heading of the robot is defined as the direction in which the robot moves. Since a DDR can move forward and backward at a point, the heading angle with respect to the robot's x-axis is zero or π.

In this paper, we will use polar coordinates to represent the position of the center of the robot in the Cartesian plane by introducing the following transformations:

$$r = \sqrt{x^2 + y^2}, \quad \theta = \tan^{-1} \frac{y}{x}. \tag{1}$$

In polar coordinates, the configuration of the robot can be represented by (r, θ, ψ).

The camera is positioned so that the optical center lies directly above the origin of the robot's local coordinate frame. The optical axis is parallel to the world $x - y$ plane, and the pan angle ϕ is the angle from the robot's x-axis to the optical axis. We assume that the range of camera rotation is limited, such that $\phi \in [\phi_1, \phi_2]$. Without loss of generality, we place the (static) landmark at the origin of the world coordinate system. These conventions are illustrated in Fig. 1.

Given this formulation, the problem that we consider is that of finding minimal-length paths from initial to goal position, such that the following conditions are satisfied.

- The camera always points toward the landmark

$$\psi + \phi = \pi + \theta. \tag{2}$$

- The camera pan angle limits are not exceeded

$$\phi \in [\phi_1, \phi_2]. \tag{3}$$

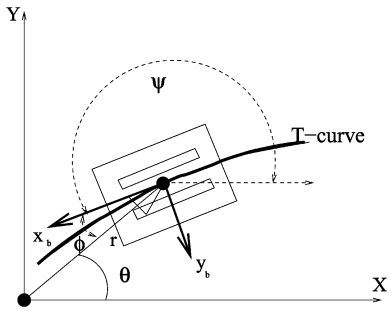

Fig. 3. T-curve construction.

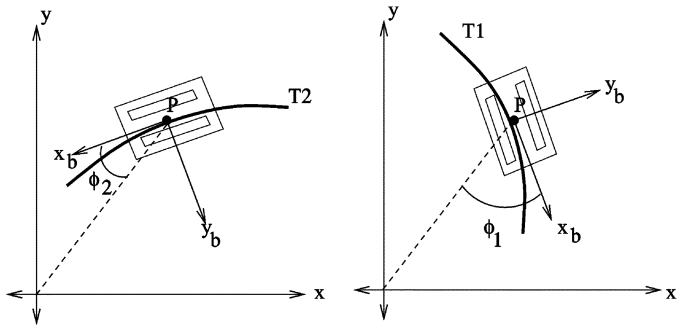

Fig. 4. (left) T2 curve. (right) T1 curve passing through P.

In the following, we assume that $0 \in [\phi_1, \phi_2]$, i.e., that the camera is pointed forward, and hence, the DDR can directly approach the landmark.

III. Controllability

In this section, we address the issue of controllability of our system. Controllability of a system is defined as its ability to reach any given admissible goal configuration in its configuration space, from any given admissible initial configuration in its configuration space using a bounded control in finite time.

Controllability of our system is important for two reasons. First, shortest paths between any two given configurations in the state space can be obtained only when the system can be driven from one configuration to the other using bounded control input. Second, the paths used to prove the controllability of the system in a constructive way also help us in finding the nature of shortest paths in Section IV.

Our proof relies on the construction of what we call T-curves, trajectories that saturate the camera pan angle. In the following, we derive these curves and use them to prove controllability. The controllability of our system holds, even in the presence of a finite range of vision of the camera, as we show in Section III-C.

A. T-Curves

Consider the curve traced out by the DDR through a generic point (r_0, θ_0) in the plane, respecting the constraint that the angle between the velocity of DDR (i.e., tangent to the curve) and the optical axis of the camera is held at a constant ϕ. To satisfy (2), the optical axis of the camera should always be pointing toward the landmark, located at the center of the circle. We refer to such a curve as a T-curve.

Proposition 1: The equation of the T-curve passing through the point (r_0, θ_0) with fixed pan angle ϕ is given by

$$r = r_0 e^{(\theta_0 - \theta)/(\tan\phi)}. \tag{4}$$

Proof: Refer to Fig. 3. Let (r_0, θ_0) be the coordinates of the point through which the curve passes. Let (r, θ) be the coordinates of a general point on the curve.

From [24], the differential equation of a planar curve is given in polar coordinates by

$$\frac{1}{r}\frac{dr}{d\theta} = -\cot\phi$$
$$\frac{1}{r}dr = -\cot\phi d\theta$$

in which ϕ is the angle between the radius and the tangent to the curve. Integrating both sides, we obtain

$$\int_{r_0}^{r} \frac{1}{r} dr = \int_{\theta_0}^{\theta} -\cot\phi d\theta.$$

Since ϕ is a constant in our case, we can take it outside the integral sign to obtain

$$\ln\frac{r}{r_0} = (\theta_0 - \theta)\cot\phi. \tag{5}$$

On simplification, we obtain

$$r = r_0 e^{(\theta_0 - \theta)/(\tan\phi)}. \tag{6}$$

■

Since ϕ is allowed to take values in $[\phi_1, \phi_2]$, two curves can be drawn through any point in the plane such that ϕ takes the values at the extremities of the interval. These curves can be thought of as latitudes and longitudes. We refer to these curves as T1 and T2 curves, when $\phi = \phi_1$ and $\phi = \phi_2$, respectively. These are illustrated in Fig. 4.

If $-\pi/2 < \phi_i < 0$, increasing θ causes r to grow. If $0 < \phi_i < \pi/2$, increasing θ causes r to decrease. Hence, when $-\pi/2 < \phi_1 < 0$ and $0 < \phi_2 < \pi/2$, we can spiral out by following the T1 curve, and spiral in by following the T2 curve in an anticlockwise sense. Or, we can spiral in by following the T1 curve, and spiral out by following the T2 curve in a clockwise sense.

B. Constructive Proof of Controllability

In this section, we present the proof of controllability of the system.

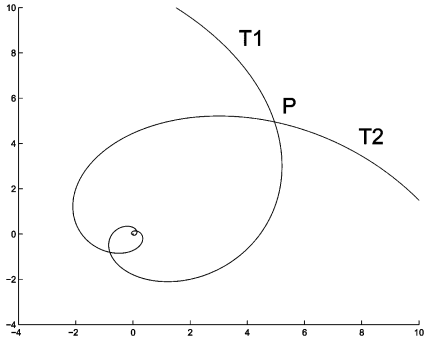

Fig. 5. When $\phi_1 \neq \phi_2$, two T-curves have infinitely many intersection points.

1) Property 1: If $\mid \phi_2 - \phi_1 \mid < \pi$ and $\phi_2 \neq \phi_1$, any T1 curve intersects any T2 curve.

Proof: We prove the property by finding one such intersection point. Let $P = (r_1, \theta_1)$ and $Q = (r_2, \theta_2)$ be any two points in the plane. By *Proposition 1*, the equation of a T1 curve passing through P is

$$r = r_1 e^{(\theta_1 - \theta)/(\tan \phi_1)}. \tag{7}$$

The equation of a T2 curve passing through Q is

$$r = r_2 e^{(\theta_2 - \theta)/(\tan \phi_2)}. \tag{8}$$

Taking the natural logarithm of both sides of (7) and (8), and then taking their difference and simplifying gives

$$r = r_1^{(\tan \phi_1)/(\tan \phi_1 - \tan \phi_2)} r_2^{(\tan \phi_2)/(\tan \phi_2 - \tan \phi_1)} \times e^{(\theta_1 - \theta_2)/(\tan \phi_1 - \tan \phi_2)}. \tag{9}$$

If $\mid \phi_2 - \phi_1 \mid < \pi$ and $\phi_1 \neq \phi_2$, r is finite.

In general, there will be infinitely many intersection points for two T-curves. These can be found by replacing either of θ_i in (9) by $\theta_i + 2k\pi$ for $k = 1, 2, \ldots$. Intersecting T-curves are shown in Fig. 5. ■

Proposition 2: The DDR is controllable between any two admissible configurations.

Proof: Let P and Q be two points in the work space. Let R be the intersection of the T1 curve from P and the T2 curve from Q. Let the DDR start at P in any configuration satisfying the constraints (2) and (3). Now rotate the DDR at P so that the angle between the robot's x-axis and the radius vector, ϕ, becomes ϕ_1. Now move along the T1 curve until the DDR reaches R. At R, the DDR rotates so that ϕ increases from ϕ_1 to ϕ_2. Now the DDR moves on the T2 curve to reach Q.

By *Proposition 1*, if $\mid \phi_2 - \phi_1 \mid < \pi$, then R exists. Since the choice of P and Q is arbitrary, the system is controllable in the case $\mid \phi_2 - \phi_1 \mid < \pi$.

If $\mid \phi_2 - \phi_1 \mid \geq \pi$, then the available velocities at any point span the plane, and controllability is immediate. ■

C. Controllability in the Presence of Bounds On Camera Range

The system is controllable even for the case in which the camera will have a finite range $r_{\max}$, beyond which it cannot detect the landmark. Thus, while navigating, the distance from the robot to the landmark must be no greater than $r_{\max}$. We may also assume that the robot must maintain some minimum distance $r_{\min}$ from the landmark (e.g., to avoid collision or to respect depth-of-field constraints). Thus, the DDR must remain in the disk $\Omega = \{(r, \theta) : r_{\min} \leq r \leq r_{\max}\}$ for successful landmark tracking. We now prove that the system is controllable in Ω; i.e., we can drive the DDR from any given initial configuration to any given final configuration in Ω, maintaining visibility of the landmark throughout the motion. It is possible to concatenate a sequence of T-curves that remain inside Ω to create what we refer to as an S-curve. The procedure for doing so is iterative, and the ith segment in the S-curve consists of a T1 segment followed by a T2 segment. There are four possible strategies, corresponding to whether we increase or decrease θ as we build the S-curve, and to whether we begin with a T1 or T2 curve. Of these four strategies, only two generate unique S-curves (the other two strategies merely traverse the curves in the opposite sense). Thus, for any $q = (r, \theta, \psi)$, there exist exactly two unique S-curves. If we begin with a T2 curve and use decreasing values of θ, the procedure begins by tracing the T2 curve through q, until $r = r_{\max}$. From this point, trace a T1 curve until $r = r_{\min}$. From this point, trace a T2 curve until $r = r_{\max}$, etc. Such an S-curve is shown in Fig. 6, with $\phi_1 = -\pi/6$ and $\phi_2 = \pi/6$.

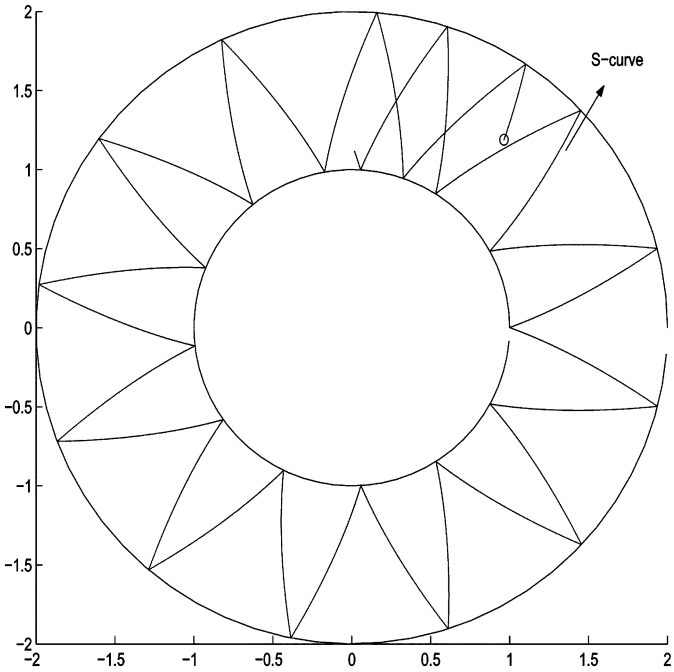

Fig. 6. S-curve for a camera angle of $+\pi/6$ and $-\pi/6$.

S-curves possess a number of interesting properties.

- The two S-curves S_1 and S_2 through any two distinct points in Ω are equivalent to each other in that they differ only by a rotation.
- Any two distinct S-curves must have at least one intersection. This can be seen from Fig. 6. A detailed proof is given in [25].
- Suppose the two S-curves S_1 and S_2 intersect at the point (r, θ). Without loss of generality, assume that at (r, θ), the

camera pan angle is $\phi = \phi_1$ for S_1, and $\phi = \phi_2$ for S_2. If the robot is following S_1, at this intersection point it can depart S_1 and begin to follow S_2. This is achieved by stopping at (r, θ) and changing the orientation so that ϕ changes from ϕ_1 to ϕ_2.

In the next proposition, we demonstrate the constructive proof of controllability.

Proposition 3: If $\phi_1 \neq \phi_2$, i.e., the camera is allowed to rotate in a closed interval of measure greater than zero, then the system is controllable in the presence of bounds on camera range.

Proof: If we have $\phi_1 = \phi_2$, then only one type of T-curve can be made, and hence, the S-curves collapse to a set of nonintersecting curves in Ω. Moreover, these S-curves are the only curves along which the DDR could move. Since the curves are nonintersecting in Ω, the system is no more controllable in this case.

If the camera is allowed to rotate in any closed interval of measure greater than zero, then we can obtain the range $[\phi_1, \phi_2]$ with $\phi_1 \neq \phi_2$. Let $q_i = (r_i, \theta_i, \phi_i)$ and $q_f = (r_f, \theta_f, \phi_f)$ be two admissible configurations of the DDR. Let q_i denote the initial configuration, and q_f denote the final configuration. Construct two S-curves in Ω, S_1 passing through (r_i, θ_i) and S_2 passing through (r_f, θ_f). Without loss of generality, assume that both S_1 and S_2 are constructed by beginning with a T2 curve and using decreasing θ.

The S-curves are distinct if q_f does not lie on S_1. If q_f does lie on S_1, then S_1 trivially defines a path from q_i to q_f.

Suppose now that S_1 and S_2 are distinct. A path from q_i to q_f can be constructed as follows. First, rotate in place until $\phi = \phi_2$ (this implicitly defines the value of ψ, since (2) must be satisfied). Now, follow S_1 until its first intersection with S_2. At this intersection point, begin to follow S_2. This requires the robot to stop at the intersection point and change its orientation so that ϕ changes from ϕ_2 to ϕ_1, or vice versa, depending on whether this intersection is an intersection of a T1 curve for S_1 and a T2 curve for S_2, or a T2 curve for S_1 and a T1 curve for S_2 (it is not possible for two T1 curves to intersect, or for two T2 curves to intersect). Finally, when the robot reaches the goal position, change the orientation such that $\psi = \psi_f$. Hence, for any feasible q_i and q_f, there exists a path from q_i and q_f satisfying the visibility constraint (2) and respecting the constraint on camera motion (3). Hence, the system is controllable.

The above argument holds if $| \phi_2 - \phi_1 | < \pi$. If $| \phi_2 - \phi_1 | \geq \pi$, then the available velocities at any point span the plane and controllability is immediate. ■

IV. Properties of Shortest Paths

In this section, we derive several properties that must be satisfied by minimal-length paths between two points in the plane for the DDR when there are no range constraints on the sensor. As a consequence of these properties, we will be able to partition the plane into eight disjoint regions, in which the structure of shortest paths is invariant for a specified initial point P. These regions are illustrated in Fig. 7. The curves partitioning the plane are the two T-curves passing through P, the two rays emanating from P that are tangent to these two T-curves at P, and the arcs of the two circles tangent to the two T-curves at P.

We denote by $\mathrm{T1}_P$ and $\mathrm{T2}_P$ the T1 and T2 curves, respectively, through the point P. We can see that $\mathrm{T1}_P$ and $\mathrm{T2}_P$ divide the plane around P into four disjoint regions, irrespective of the numerical values of ϕ_1 and ϕ_2. We have followed a nomenclature of naming those regions as shown in Fig. 8. The line from the landmark to the point P passes through two of these regions. One of those regions contains the landmark and is called the D-type region, and the other region is called the C-type region. The remaining two regions are given the names A and B, as shown in Fig. 8. Since the camera is pointing forward, the possible heading of the robot from P can only be into region C or C. Based on these regions, we define four kinds of nondifferentiable points in a path that transitions from one T-curve to another: Type A', Type B', Type C', and Type D'. These are shown in Fig. 9.

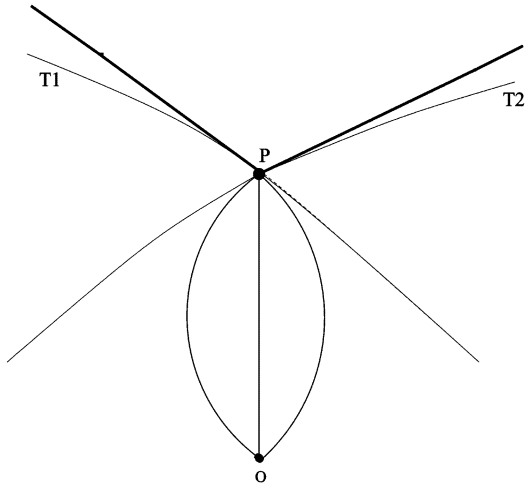

Fig. 7. Partition of the plane at P into eight regions that define invariant classes of shortest paths.

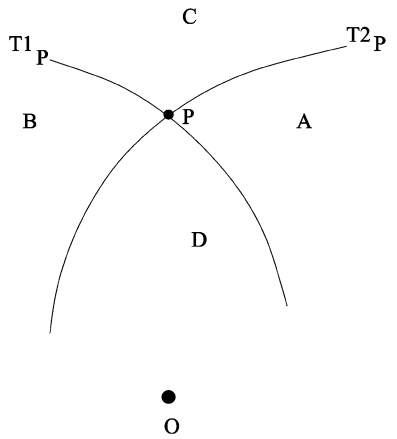

Fig. 8. Division of the plane at P by T-curves.

We now present several properties of the shortest paths along with their proofs.

Let P be the initial point and O be the landmark, as shown in Fig. 10. The line PO divides the plane into the two half-planes P^+ and P^-. Let Q be the goal point.

1) Property 2: A minimal-length path for the DDR from P to Q that respects the constraints (2) and (3) never crosses the line PO. The minimal-length path from P to any point Q on the line PO is the straight line PQ.

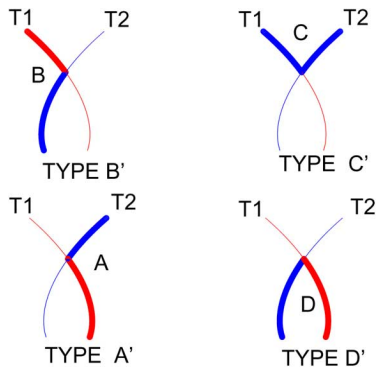

Fig. 9. Type of nondifferentiable points on the path.

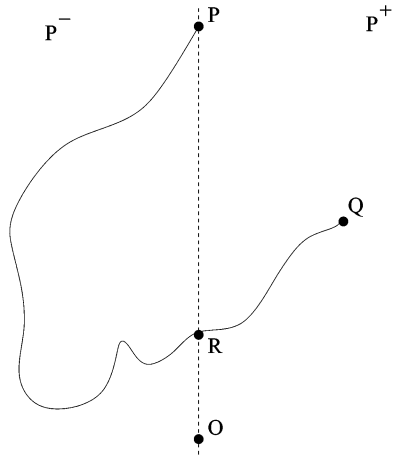

Fig. 10. P is the initial point. O is the landmark. The line PO divides the plane into two half-planes P^+ and P^-. Q is the goal point.

Proof: Refer again to Fig. 10. Suppose the minimal-length path L intersects the line PO at a point R. If L is minimal length, then the part of the path from P to R on L also must be minimal length. But the minimal-length path from P to any point R on this line is the straight line from P to R, since the DDR can move straight toward and away from the landmark. Hence, if Q does not lie on the line PO, L can never intersect the line PO. From the construction, it can be trivially seen that if Q lies on line PO, then the minimal-length path from P to Q is the straight line PQ. ■

We define the S-set of a point P to be the set of points that can be reached on a straight-line path from P without violating constraints (2) and (3). In the next two properties, we present a derivation for the shape of the S-set.

2) Property 3: If the robot heading at the point P points into a region of type D, then the S-set is the region bounded by the arc of circles tangent to $\mathrm{T1}_P$ and $\mathrm{T2}_P$ at P, and passing through the origin O. This is shown in Fig. 11.

Proof: Refer to Fig. 12. Since the robot is heading into a region of type D, the angle between its heading and the radius vector is given by ϕ. Let the robot start heading on a straight line from the initial point P in a direction such that $\phi \in [0, \phi_2]$. Let R denote the position of the robot as it moves forward along the line PT. Then ϕ is $\angle ORT$. It can be seen from the figure that as length PR increases, $\angle ORT$ increases. Hence, the robot can move only until it reaches the point $R = Q$ such

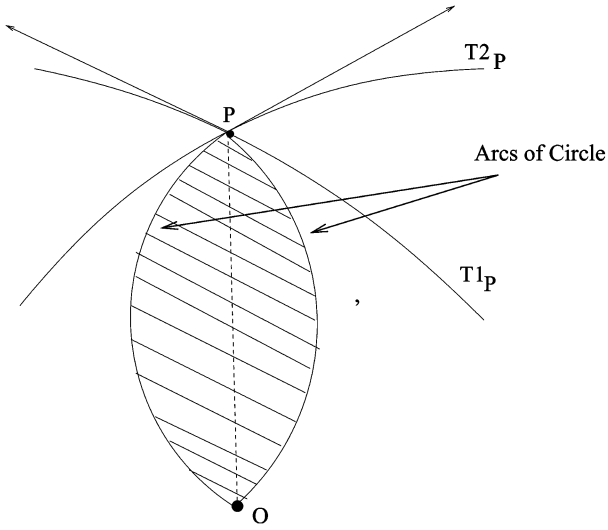

Fig. 11. Lower portion of the S-set for point P.

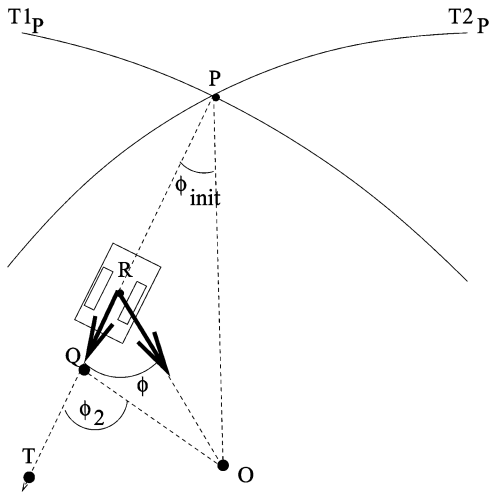

Fig. 12. S-set derivation for region of type D.

that $\angle OQT = \phi_2$. This is true for any $\phi \in [0, \phi_2]$. Hence, the end point Q on PT satisfies the constraint $\angle OQT = \phi_2$. From known properties of circles, we conclude that the locus of point Q is an arc of a circle circumscribing $\triangle PQO$, and also that the tangent at P to the arc OQP makes an angle of ϕ_2 with the line segment PO, which is the same as the tangent to the T2 curve at P. Hence, arc OQP and $\mathrm{T2}_P$ share the same tangent at P. Similarly, if $\phi \in [\phi_1, 0]$, the locus of Q' is the arc of the circle circumscribing $\triangle PQ'O$ such that $\angle OQ'T = \phi_1$ and the arc $OQ'P$ and $\mathrm{T2}_P$ share the same tangent at P. Hence, the S-set in this case includes the union of sectors of two circles, as shown in Fig. 11.

3) Property 4: If the robot heading from the point P is in the region of type C, then the S-set is the region bounded by the lines tangent to $\mathrm{T1}_P$ and $\mathrm{T2}_P$ at P. This is illustrated in Fig. 13.

Proof: Refer to Fig. 14. Let the robot start heading on a straight line in a region of type C from P, in a direction such that $\angle OPT = \alpha$. Let R denote the position of the robot as it moves forward along the line PT. As the robot moves ahead along PT, $\angle ORT$ increases if $\alpha \leq \pi$, and decreases if $\alpha \geq \pi$.

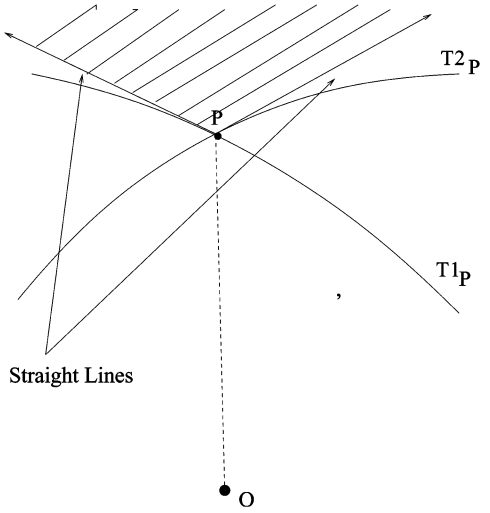

Fig. 13. Upper portion of the S-set for point P.

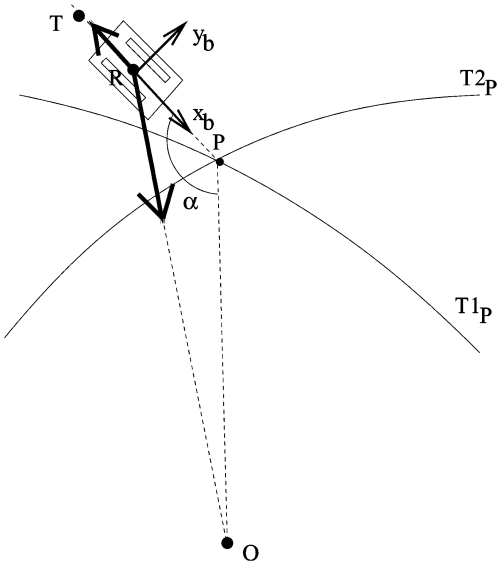

Fig. 14. S-set derivation for region of type C.

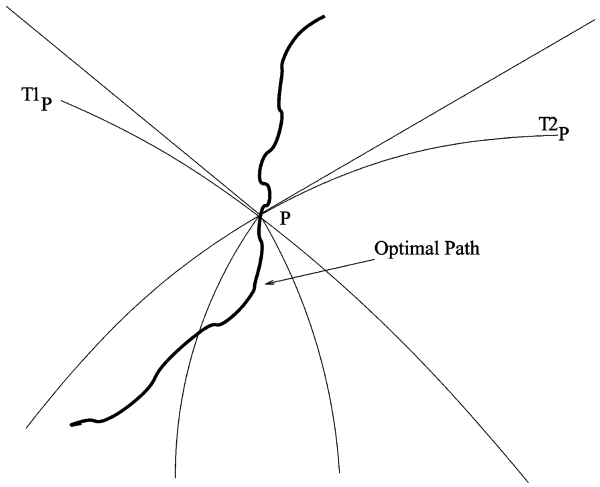

Fig. 15. Candidate shortest path through the point P that is neither a straight+line segment nor a T-curve.

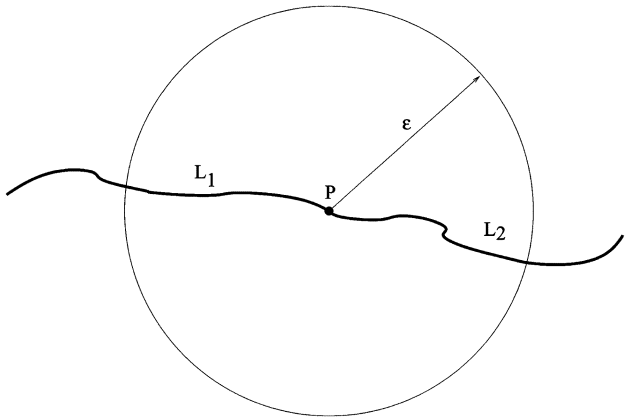

Fig. 16. Shortest path through point P.

As the robot moves to infinity on line PT, α tends to π, which, in turn, implies that ϕ tends to zero. Hence, there is no constraint on the limit to which the robot can move. The S-set in this case includes the region enclosed by the rays PA and PB, as shown in Fig. 13.

The next property shows that shortest paths are obtained by concatenating T-curves and straight lines.

4) Property 5: Shortest paths for the DDR that respect the constraints (2) and (3) consist of straight-line segments and sections of T-curves.

Proof: Suppose that the shortest path contains a curve that is neither a straight line nor a T-curve. In this case, there must exist a point P on the curve such that the shortest path is not a T-curve at P (the tangent to the shortest path at P does not make an angle of ϕ_1 or ϕ_2 with radial line), nor is it a straight line at P. The shortest path passes through P, as shown in Fig. 15. Since the shortest path passes through the S-set (and is not tangent to the boundary, since it is not the T-curve at P), any point in the intersection of the shortest path and the S-set can be reached by a straight line from P. Since the shortest path is not a straight line at P, the above path ceases to be a shortest path, since it can be shortened by a straight line in a neighborhood of P.

Now we present a property that characterizes nonsmooth points on shortest paths.

5) Property 6: For a C^0 path to be minimal length, the nondifferentiable points on the path can only be of Type C' or Type D'.

Proof: Refer to Fig. 16. We impose the restriction on admissible paths that the set of nondifferentiable points along the path be countable. If this condition were violated, in practice, a robot could not traverse the path. Since we show in the folowing that this class of admissible paths contains the minimal-length paths, this restriction does not pose any problem for our method.

Let the minimal-length path be denoted by L. Take a ball of radius ϵ around a nondifferentiable point P on L. Denote it by B_ϵ. Consider the part of L inside B_ϵ. This can be denoted as $B_\epsilon \cap L$. Now P divides $B_\epsilon \cap L$ into two smaller segments, L_1 and L_2. Hence, $B_\epsilon \cap L - \{P\} = L_1 \cup L_2$. Since the set of nondifferentiable points on L is countable, we can find an $\epsilon > 0$ such that $L_1, L_2 \in C^1$.

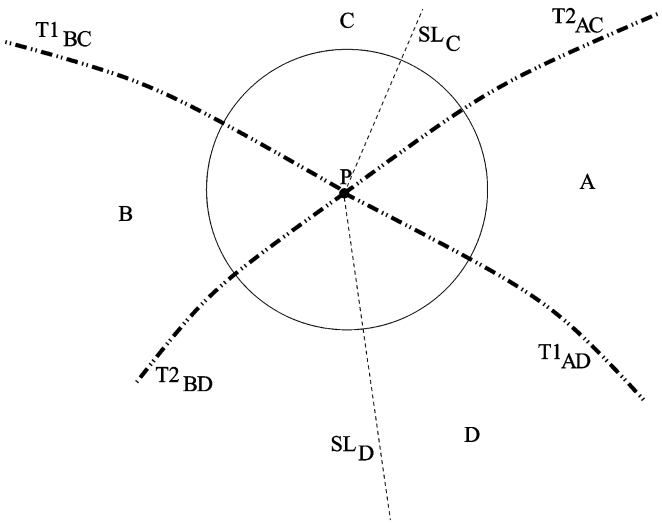

Fig. 17. Types of minimal-length paths around a nondifferentiable point.

Since L_1 and L_2 belong to C^1, by *Property 5*, if L is minimal-length, each of L_1 and L_2 is a straight line or a T-curve. Hence, we can reduce the family of minimal-length paths through P to be of the forms as shown in Fig. 17, in which the following notation is adopted:

- $SL_{\rm C}$—Straight line in region of type C;
- $SL_{\rm D}$—Straight line in region of type D;
- $\mathrm{T2}_{\rm AC}$—T2 curve separating regions A and C;
- $\mathrm{T1}_{\rm AD}$—T1 curve separating regions A and D;
- $\mathrm{T1}_{\rm BC}$—T1 curve separating regions B and C;
- $\mathrm{T2}_{\rm BD}$—T2 curve separating regions B and D.

Therefore, the problem has been reduced to eliminating those cases in which the path can be shortened, respecting the constraints of the DDR. From Fig. 17, we can enumerate the following 15 cases:

1) $SL_{\rm C} \leftrightarrow \mathrm{T1}_{\rm AD}$;
2) $SL_{\rm C} \leftrightarrow \mathrm{T1}_{\rm BC}$;
3) $SL_{\rm C} \leftrightarrow \mathrm{T2}_{\rm AC}$;
4) $SL_{\rm C} \leftrightarrow \mathrm{T2}_{\rm BD}$;
5) $SL_{\rm C} \leftrightarrow SL_{\rm D}$;
6) $\mathrm{T1}_{\rm BC} \leftrightarrow SL_{\rm D}$;
7) $\mathrm{T1}_{\rm AD} \leftrightarrow SL_{\rm D}$;
8) $\mathrm{T2}_{\rm BD} \leftrightarrow SL_{\rm D}$;
9) $\mathrm{T2}_{\rm AC} \leftrightarrow SL_{\rm D}$;
10) $\mathrm{T1}_{\rm BC} \leftrightarrow \mathrm{T1}_{\rm AD}$;
11) $\mathrm{T2}_{\rm BD} \leftrightarrow \mathrm{T2}_{\rm AC}$;
12) $\mathrm{T1}_{\rm AD} \leftrightarrow \mathrm{T2}_{\rm AC}$;
13) $\mathrm{T2}_{\rm BD} \leftrightarrow \mathrm{T1}_{\rm BC}$;
14) $\mathrm{T1}_{\rm BC} \leftrightarrow \mathrm{T2}_{\rm AC}$;
15) $\mathrm{T2}_{\rm BD} \leftrightarrow \mathrm{T1}_{\rm AD}$.

We first describe the shortening of the paths for cases 1–5. Consider Fig. 18, in which $I, F \in B_\epsilon$ are the initial and final points of a path segment under consideration. Consider a point U on $SL_{\rm C}$. Since there is a straight line from U to P, P lies in the S-set of U. Since the S-set for a point U includes an open set bounded by the arcs of two circles (recall Figs. 11 and 13), for some U very close to P, there is a neighborhood of P, B_P, that lies in the S-set of U. B_P intersects with $\mathrm{T1}_{\rm AD}$, $\mathrm{T1}_{\rm BC}$, $\mathrm{T2}_{\rm AC}$, $\mathrm{T2}_{\rm BD}$, and $SL_{\rm D}$ at $V_{\rm AD}$, $V_{\rm BC}$, $V_{\rm AC}$, $V_{\rm BD}$, and $V_{\rm D}$, respectively. Since $V_{\rm AD}, V_{\rm BC}, V_{\rm AC}, V_{\rm BD}$, and $V_{\rm D}$ lie in the S-set of U, straight lines can be drawn from U to to each of them, and this shortens the path for each of the above cases. The shortening of the path is shown by the dashed lines.

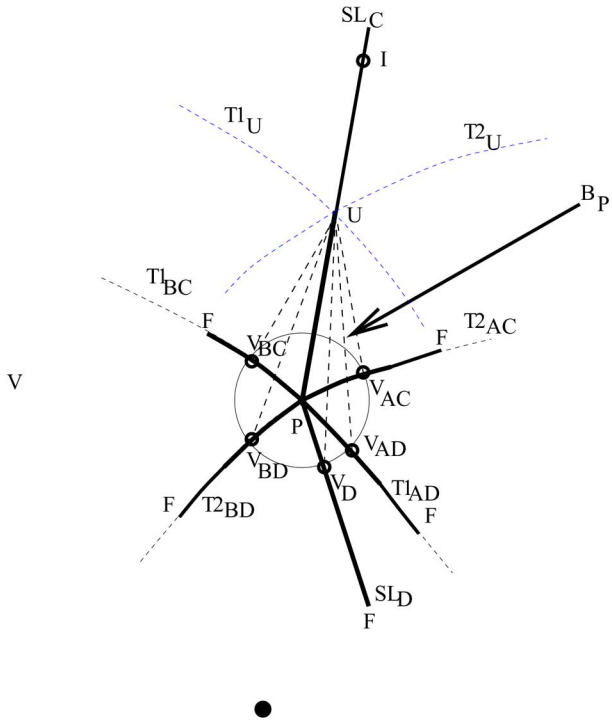

Fig. 18. Shorter paths for cases 1–5.

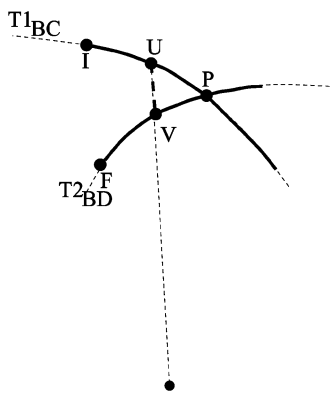

Fig. 19. Shorter paths for cases 12 and 13.

Cases 6–9 can be shortened in the same manner.

For cases 10 and 11, P is not a nondifferentiable point, and therefore, these cases are not relevant to *Property 6*.

Now let us consider the cases 12 and 13. Consider the path $\mathrm{T2}_{\rm BD} \leftrightarrow \mathrm{T1}_{\rm BC}$. Refer to Fig. 19, again with $I, F \in B_\epsilon$ the initial and final points of a path segment under consideration. The DDR can move on a straight line from the point U on $\mathrm{T1}_{\rm BC}$ to the origin, and this intersects $\mathrm{T2}_{\rm BD}$ at the point V. The dashed line UV shortens the path $\mathrm{T2}_{\rm BD} \leftrightarrow \mathrm{T1}_{\rm BC}$. The same arguments can be applied to $\mathrm{T1}_{\rm AD} \leftrightarrow \mathrm{T2}_{\rm AC}$.

The only cases that remain are that of $\mathrm{T1}_{\rm BC} \leftrightarrow \mathrm{T2}_{\rm AC}$ and $\mathrm{T2}_{\rm BD} \leftrightarrow \mathrm{T1}_{\rm AD}$, which correspond to a nondifferentiable point

of the types C' and D', respectively. Hence, for C^0 paths to be minimal-length, any nondifferentiable point has to be of the type C' or D'. ■

In the next section, we give an explicit enumeration of the types of minimal-length paths possible.

V. The Language of Shortest Paths

From the properties derived in the earlier section, we conclude that the minimal-length paths include only segments that are T-curves and straight lines (denoted, respectively, by T1, T2, and SL). In the case of a C^0 path, the nondifferentiable points can be only of Type C' or Type D'. We represent a path by a string (or a *word*) of the form $X_1 - X_2 * X_3 \cdots X_n$, where each X_i is one of T1, T2, or SL, and where the symbol "$-$" denotes a smooth transition between segments and the symbol "$*$" denotes a nonsmooth transition. For example, $SL-$T1 implies that SL is tangent to T1 at the point of contact, whereas $SL*$T1 denotes that SL is not tangent to T1 at the point of contact. Due to the kinematic constraints of the DDR and the properties of shortest paths, only a subset of possible words are included in the language of shortest paths. The following lemma makes this set explicit.

Lemma 1: If a straight line is present in the shortest path, then the words $SL -$ T1 $- SL$, $SL -$ T2 $- SL$, T1 $-SL-$ T2, T2 $-SL-$ T1, T2 $-SL-$ T2, T1 $-SL-$ T1, $SL -$ T2$*$ T1, and $SL -$ T1$*$ T2 are not possible.

Proof: We prove the cases individually.

1) $SL -$ T2 $- SL$: A smooth transition from T2 to SL can take place only if at the point of transition, the SL is in a region of type B or C. But heading into a region of type B is forbidden, due to camera constraints, and hence, the transition must be on an SL in a region of type C. An $SL-$T2$-SL$ path, with both SL paths in the region of type C at the point of transition, will have one transition point that is nondifferentiable. But since this nondifferentiable point is neither of the form C' nor D', the path cannot be a shortest path.
2) $SL -$ T1 $- SL$: This case is same as the above case.
3) T2 $-SL-$ T1: Refer to Fig. 20. Suppose the robot travels on a T2 curve from P to B, at which point it takes the SL path tangent to T2 at B. If the DDR is to make a C^1 transition from this SL path to a T1 curve, say at some point C, then $\angle OCB = \phi_1 < 0$. But as the DDR moves along SL, $\angle OCB$ can never decrease below zero, which it attains only in the limit as the DDR goes to infinity. Therefore, there does not exist such a transition point C.
4) T1 $-SL-$ T2: The arguments in this case are same as the arguments in the case of T2 $-SL-$ T1.
5) T2 $-SL-$ T2: Refer to Fig. 21. Suppose the robot travels on a T2 curve from P to B, at which point it takes the SL path tangent to T2 at B. If the DDR is to make a C^1 transition from this SL path to a T2 curve, say at some point C, then $\angle OCB = \phi_2$.
   But the sum of angles of the $\triangle OBC$ is equal to π. This implies that $\angle BOC = 0$. This implies that B has to coincide with C, resulting in a zero-length SL path. Therefore, there does not exist a path of the form T2 $-SL-$ T2.

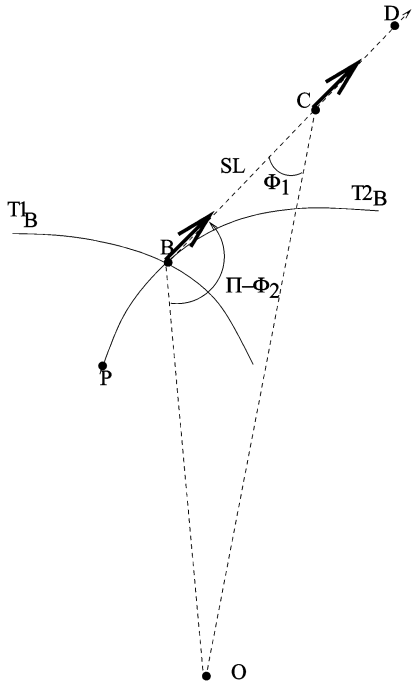

Fig. 20. Contradiction for T2 $-SL-$T1.

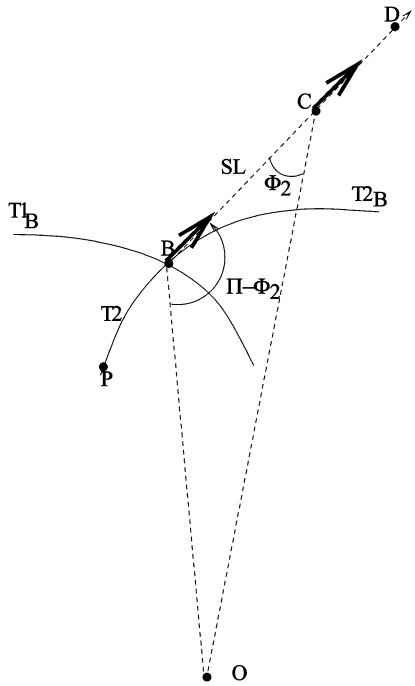

Fig. 21. Contradiction for T2 $-SL-$ T2.

6) T1 $-SL-$ T1: The arguments in this case are same as the arguments in the case of T2 $-SL-$ T2.
7) $SL -$ T2$*$ T1: Refer to Fig. 22. Consider an $SL -$ T2$*$ T1 from P to Q. PM_1' is a straight line. $M_1'M_1$ is a T2 curve. M_1, M_2, M_3, and M_4 are points on T1$_Q$. M_1', M_2', and M_3' are intersections of T2$_{M_1}$, T2$_{M_2}$, and T2$_{M_3}$ at the boundary of the S-set at P. PM_1', PM_2', PM_3', and PM_4 are straight-line segments. Suppose that the shortest path from P to Q is $PM_1'M_1Q$. Then we can further reduce the

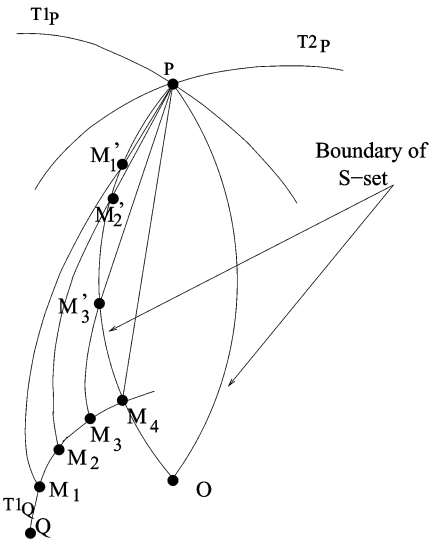

Fig. 22. Contradiction for SL − T2∗ T1.

length $PM_1'M_1$ by traveling along $M_1M_2M_2'P$ instead of $M_1M_1'P$, since $M_1M_2M_2'P$ is a path of type $SL-$T2∗ T1. If we iterate in this manner, we reach a point M_4, which is the intersection of $T1_Q$ with the boundary of the S-set at P. The point M_4 is a nondifferentiable point of the type T1 $*SL$, and hence, by *Lemma 1*, it cannot be on a shortest path from P to Q. Hence, QM_4P cannot be a shortest path from P to Q. Moreover, the $SL-$T2∗ T1 paths from P to Q are also not shortest paths, since their lengths are greater than the QM_4P path. Hence, no SL − T2∗ T1 path is a word in the language of shortest paths.

8) SL − T1∗ T2: The arguments in this case are the same as the arguments in the case of SL − T2∗ T1.

■

All remaining combinations of SL, T1, and T2 qualify to be a part of the shortest path. The remaining words are $SL-$ T1, T1 $-SL$, and $SL-$ T2. From the above properties of shortest paths, the next theorem shows that the set of acceptable words are SL, T1, T2, $SL-$ T1, T1 $-SL$, $SL-$ T2, T2 $-SL$, T1 ∗T2 ∗ T1 ∗ T2 ⋯ and T2 ∗T1 ∗ T2 ∗ T1 ⋯.

Theorem 1: The acceptable words in the language of shortest paths for a DDR that respects the constraints (2) and (3) are SL, T1, T2, $SL-$ T1, T1$-SL$, $SL-$ T2, T2$-SL$, T1∗T2 ∗ T1 ∗ T2 ⋯ and T2 ∗T1 ∗ T2 ∗ T1 ⋯.

Proof: The process of synthesizing the paths can be considered as filling the blanks with SL, T1 or T2 and literal ? by − or ∗ in _?_?_?_?. . . . . ., respecting constraints (2) and (3). Apart from all the theorems proved till now, the shortest paths cannot consist of a nonsmooth transition from T1 to T1, T2 to T2, and SL to SL. Moreover, there can be no transitions of the form T1 − T2 or T2 − T1.

If the shortest paths consist of only one type of segment (or equivalently, filling up just one blank), then it can only be SL, T1, or T2, as proved in *Property 5*.

If the shortest paths consist of two kinds of segment, then an equivalent problem consists of number of ways to fill _?_. If ? is a −, then the paths are $SL-$ T1, T1 $-SL$, $SL-$ T2, T2 $-SL$. If ? is a ∗, the only allowed paths are T1 ∗ T2 and T2 ∗ T1 by *Property 6*.

If the shortest paths consist of three kinds of segment, then an equivalent problem consists of the number of ways to fill _?_?_. If any _ is filled by SL, then the ? adjacent to it cannot be ∗. Moreover, *Lemma 1* eliminates all the rest of the paths in which SL can be present. Hence, SL cannot be present in a shortest path with three different kinds of segments. The only ways in which T1 and T2 can be allowed to fill up the blanks are T1 ∗T2∗ T1 and T2 ∗T1∗ T2. Hence, these are the only ways in which a shortest path can be formed with three different kinds of segments.

Now consider the case in which there are four or more different types of segments forming the shortest paths. Every subpath of a shortest path is a shortest subpath. Hence, SL cannot be present, since there is no shortest subpath consisting of three different segments that has SL in it. The only way to fill up the _ is by using T1 and T2 alternately, and filling the ? by ∗. In the case in which there are four or more different types of segments forming the shortest paths, the only possibility is T1 ∗T2 ∗ T1 ∗ T2 ⋯ and T2 ∗T1 ∗ T2 ∗ T1 ⋯.

Hence, the acceptable words are SL, T1, T2, $SL-$ T1, T1 $-SL$, $SL-$ T2, T2$-SL$, T1 ∗T2 ∗ T1 ∗ T2 ⋯ and T2 ∗T1 ∗ T2 ∗ T1 ⋯. ■

Summarizing, the acceptable words are SL, T1, T2, $SL-$ T1, T1 $-SL$, $SL-$ T2, T2 $-SL$, T1 ∗T2∗ T1 ∗T2 ⋯ and T2 ∗T1 ∗ T2 ∗ T1 ⋯. The last two words can consist of any number of repetitions as long as the transition from one T-curve to another T-curve occurs through a Type C' or Type D' point. In the next section, we present the partition of the space of reachable points from P using the set of words in the language of shortest paths.

VI. Synthesis of Shortest Paths

For a starting point P in the plane for a DDR, the words in the language of shortest paths induce a partition of the plane into regions, such that a specific word corresponds to the shortest path to any goal point Q in a region. This partition is illustrated in Fig. 23, in which the regions are given labels that are used in the discussion that follows. We note that the topology of this partition does not change as the values of ϕ_1 and ϕ_2 vary, so long as we maintain the conditions that $\phi_1 \neq \phi_2$, $0 \in [\phi_1, \phi_2]$, and $|\ \phi_2 - \phi_1\ | < \pi$. We now enumerate the possible words and identify the regions in which each applies.

A. SL Region (Regions I and I')

The shortest paths from P to any point in the S-set are straight lines. The S-set of the point P gives the region consisting of points that are reachable by SL.

B. T Region (T1, T2 Curves)

$T1_P$ and $T2_P$ are the curves that are obtained by following the words T1 and T2 from P.

C. SL-T1 Region (Region II)

Consider a straight line from P to a point U that lies at the boundary of the S-set in Region I'. The transition from the straight-line path PU to $T1_U$ is C^1 [25]. All points lying on $T1_U$ are reachable by the word $SL-$ T1. The loci of points on

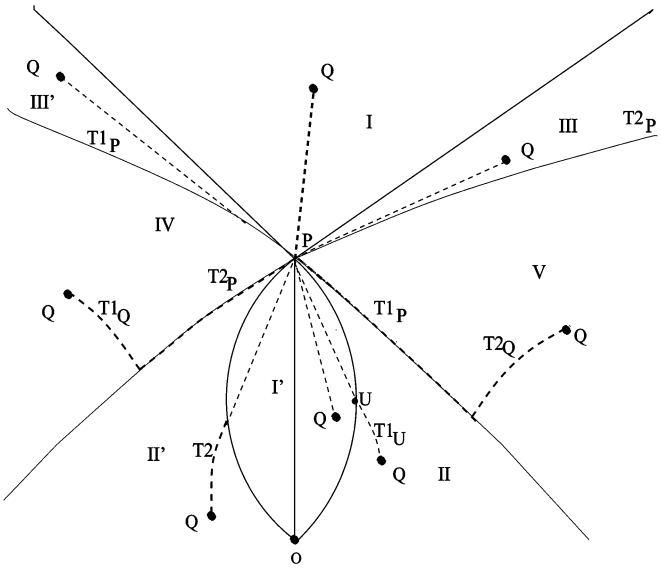

Fig. 23. Shortest paths.

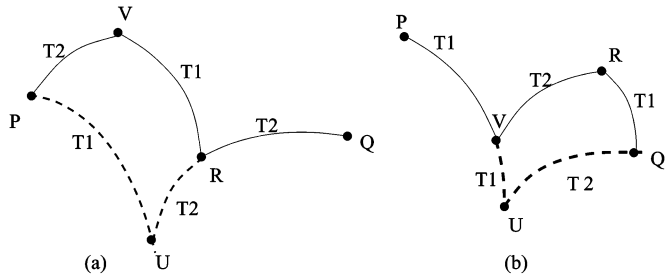

Fig. 24. Path shortening for $n = 2$. (a) Case of $T2 * T1 * T2$, and (b) case of $T1 * T2 * T1$.

$\mathrm{T1}_U$ obtained by moving U over the boundary of the S-set of P forms Region II.

D. SL-T2 Region (Region II')

Region II' is obtained in a manner similar to that used to derive Region II.

E. T2-SL Region (Region III)

If the shortest path from P to Q is of the form T2 $-SL$, then P lies in Region II' with respect to Q. Hence, the Region III of P consists of all those points Q for which P belongs to Region II' of Q.

F. T1-SL Region (Region III')

Region III' is obtained in a manner similar to that used to derive Region III.

G. T2 *T1 * T2 ... Region (Regions IV and V)

The points reachable by using the word T1 $*$T2 $*$ T1 $*$ T2 ... lie in Regions V and VI. This is due to the underlying fact that the point on the shortest path at which the transition T1 $*$ T2 or T2 $*$ T1 takes place must be of Type C' or Type D'.

H. T1 *T2 * T1 ... Region (Regions IV and V)

The analysis for T1 $*$T2 ... also holds true for this region, and hence, the reachable set of points from P remains the same.

The above analysis provides an exhaustive enumeration of the possible cases. The only regions for which more than one word is possible are Regions IV and V. It can be shown that $\mathrm{T1}_P * \mathrm{T2}_Q$ is shorter than $\mathrm{T2}_P * \mathrm{T1}_Q$ [25]. This is the main idea used to prove the next theorem. We show that given a path of the form T1 $*$T2 $*$ T1 $*$ T2 ... or T2 $*$T1 $*$ T2 ... from P to Q with an arbitrary number of nondifferentiable points, $\mathrm{T1}_P * \mathrm{T2}_Q$ is shorter in length. Since we prove this for a path with an arbitrary number of nondifferentiable points, it implies that the shortest path in the family of T1 $*$T2 $*$ T1 $*$ T2 ... and T2 $*$T1 $*$ T2 ... is $\mathrm{T1}_P * \mathrm{T2}_Q$. Since the shortest path in this region has to be the shortest path belonging to the family of T1$*$T2$*$T1$*$T2 ... and T2 $*$T1 $*$ T2 ..., we see that $\mathrm{T1}_P * \mathrm{T2}_Q$ is the shortest path.

Theorem 2: If Q lies in a region of type A, $\mathrm{T1}_P * \mathrm{T2}_Q$ is not longer than any path of the form T1 $*$T2 $*$ T1 $*$ T2 ... or T2 $*$T1 $*$ T2 ... from P to Q with a countable number of nondifferentiable points.

Proof: We prove this by induction on the number of nondifferentiable points between P and Q. Let n be the number of nondifferentiable points between P and Q.

- Base Case: For $n = 1$, it can be shown that $\mathrm{T1}_P * \mathrm{T2}_Q$ is shorter than $\mathrm{T2}_P * \mathrm{T1}_Q$ [25]. For $n = 2$, refer to Fig. 24. There are two possible cases: T1 $*$T2$*$ T1 or T2 $*$T1$*$ T2. Let us consider the case of T1 $*$T2$*$ T1 shown by Fig. 24(b). In Fig. 24(b), the path T2 $*$ T1 from V to Q can be shortened by replacing it by a T1 $*$ T2 path, as shown by the dashed lines. Finally, a shorter path from P to Q is $\mathrm{T1}_P * \mathrm{T2}_Q$. The argument is similar for the case of T2 $*$T1$*$ T2, as shown in Fig. 24(a). Hence, the shortest path with two maximum nondifferentiable points is $\mathrm{T1}_P * \mathrm{T2}_Q$.
- Induction Hypothesis: If a maximum of k transitions is allowed between T1 and T2 on a path from P to Q, then the shortest path from P to Q is $\mathrm{T1}_P * \mathrm{T2}_Q$.
- Induction Step: Let $P_1, P_2, \ldots, P_k, P_{k+1}$ be the sequence of nondifferentiable points of type C' or D' on the path from P to Q. Hence, the entire path can be denoted as $PP_1P_2..P_k, P_{k+1}Q$. Since the path from P to P_{k+1} consists of k nondifferentiable points, by the induction hypothesis, a shorter path from P to P_{k+1} is $\mathrm{T1}_P$$*$$\mathrm{T2}_{P_{k+1}}$. The entire path can be shortened to $\mathrm{T1}_P * \mathrm{T2}_{P_{k+1}} * \mathrm{T1}_Q$. Now we can apply the case for $n = 2$ and further shorten the path to $\mathrm{T1}_P * \mathrm{T2}_Q$. $\mathrm{T1}_P * \mathrm{T2}_Q$ is a shorter path for a maximum of $n = k+1$ transitions between T1 and T2. By the principle of induction, the hypothesis holds for any n, which implies that $\mathrm{T1}_P * \mathrm{T2}_Q$ is shorter than T1 $*$T2$*$T1$*$T2 ... and T2 $*$T1 $*$ T2 ....

Hence we have proved the theorem. ■

Since the shortest path from P to Q belongs to the family of paths T1 $*$T2 $*$ T1 $*$ T2 ... and T2 $*$T1 $*$ T2 ..., from *Theorem 1*, we can conclude that $\mathrm{T1}_P * \mathrm{T2}_Q$ is a shortest path from P to Q. From the above facts, we can conclude that the shortest path from P to Q in Region V is $\mathrm{T1}_P * \mathrm{T2}_Q$. Similarly, the shortest path from P to Q in Region IV is $\mathrm{T2}_P * \mathrm{T1}_Q$.

Finally, the nature of shortest paths required to move from an initial point P to a final point Q in the workspace is shown in Fig. 23, and also summarized in Table I.

TABLE I
TYPES OF SHORTEST PATHS ACCORDING TO REGIONS

Region	Subregion	Type of paths
C	I	SL
C	III'	$T1_P - SL$
C	III	$T2_P - SL$
D	I'	SL
D	II'	$SL - T2_Q$
D	II	$SL - T1_Q$
A	V	$T1_P * T2_Q$
B	IV	$T2_P * T1_Q$

VII. CONCLUSION AND FUTURE WORK

In this paper, we have considered the problem of finding shortest paths for landmark-based navigation by differential-drive vehicles (i.e., vehicles that include a nonholonomic constraint, but have the capability to rotate at a point) with FOV constraints. The camera has a finite range of rotation.

We have shown that the system is controllable, even when range limitations are imposed by the vision system. We have shown that shortest paths consist of straight-line segments and curves for which the camera viewing angle is saturated, the latter corresponding to exponential spirals which we refer to as T-curves. Finally, we have developed the language of shortest paths, and given a partition of the plane such that within any region, the optimal path is either a straight-line segment or a T-curve. Transitions occur at region boundaries and may be either smooth or nonsmooth. We have shown that for shortest paths, the transitions from a T-curve to a straight-line segment or from a straight-line segment to a T-curve are smooth, while a transition from one T curve to another is nonsmooth.

We are currently pursuing research aimed at extending this work in several directions. We are interested in developing controllers capable of executing the trajectories described above. To this end, we have begun investigating hybrid-switched controller design for visual servo systems. We are also interested in deriving time-optimal paths that honor the sensing and nonholonomic constraints of our system. To find time-optimal paths, we hope to apply PMP to the constrained optimization problem presented by our system. Finally, we would like to apply our results to the problem of planning collision-free motions in an environment that contains obstacles. To do so, we hope to develop planning schemes analogous to those given in [13] or [14], but for the case in which the set of admissible trajectories is further constrained by sensor limitations.

ACKNOWLEDGMENT

The authors would like to thank the Editors and anonymous reviewers for their comments, which have greatly improved the quality of this paper. In addition, they would like to thank J.-P. Laumond for useful discussions. They would also like to thank G. Lopez-Nicolas and H.-u. Yoon.

REFERENCES

[1] J. P. Laumond, *Robot Motion Planning and Control*. Toulouse, France: Springer, 1998.

[2] L. E. Dubins, "On curves of minimal length with a constraint on average curvature and with prescribed initial and terminal position and tangents," *Amer. J. Math.*, vol. 79, no. 3, pp. 497–516, 1957.

[3] J. A. Reeds and L. A. Shepp, "Optimal paths for a car that goes both forwards and backwards," *Pacific J. Math.*, vol. 145, no. 2, pp. 367–393, 1990.

[4] L. S. Pontryagin, V. G. Boltyanskii, R. V. Gamkrelitz, and E. F. Mishchenko, *Mathematical Theory of Optimal Processes*. New York/London: Wiley, 1962.

[5] H. Sussman and G. Tang, "Shortest paths for a non-holonomic car: A worked out example of the use of geometric techniques in non-linear optimal control," Sycon 91-10, Dept. Math., Rutgers Univ., New Brunswick, NJ, 1991, Tech. Rep.

[6] J. D. Boissonnat, A. Cerezo, and J. Leblond, "Shortest paths of bounded curvature in the plane," in *Proc. IEEE Int. Conf. Robot. Autom.*, May 1992, pp. 2315–2320.

[7] P. Soueres and J. P. Laumond, "Shortest paths synthesis for a car-like robot," *IEEE Trans. Autom. Control*, vol. 41, no. 5, pp. 672–688, May 1996.

[8] M. Chyba and S. Shekhavat, "Time optimal paths for a mobile robot with one trailer," in *Proc. IEEE Int. Conf. Intell. Robot. Syst.*, Oct. 1999, pp. 1669–1674.

[9] M. Chyba, L. E. Leonard, and E. D. Sontag, "Optimality for underwater vehicles," in *Proc. IEEE Conf. Decision, Control*, Dec. 2003, pp. 4204–4209.

[10] M. Chyba, "Underwater vehicles: A surprising non-time-optimal path," in *Proc. IEEE Conf. Decision, Control*, Dec. 2003, pp. 2750–2755.

[11] M. Chyba, H. Sussmann, H. Maurer, and G. Vossen, "Underwater vehicles: The minimum time problem," in *Proc. IEEE Conf. Decision, Control*, Dec. 2004, pp. 1370–1375.

[12] A. Bicchi, G. Casalino, and C. Santilli, "Planning shortest bounded-curvature paths for a class of nonholonomic vehicles among obstacles," *J. Intell. Robot. Syst.*, vol. 16, no. 4, pp. 387–405, Aug. 1996.

[13] J. P. Laumond, P. E. Jacobs, M. Taix, and R. M. Murray, "A motion planner for nonholonomic mobile robots," *IEEE Trans. Robot. Autom.*, vol. 10, no. 5, pp. 577–593, Oct. 1994.

[14] F. Lamiraux, S. Sekhavat, and J. P. Laumond, "Motion planning and control for Hilare pulling a trailer," *IEEE Trans. Robot. Autom.*, vol. 15, no. 4, pp. 640–652, Aug. 1999.

[15] V. Isler, D. Sun, and S. Sastry, "Roadmap based persuit-evasion and collision avoidance," in *Proc. Robot.-Sci. Syst.*, Jun. 2005, pp. 257–264.

[16] D. B. Reister and F. G. Pin, "Time optimal trajectories for mobile robots with two independently driven wheels," *Int. J. Robot. Res.*, vol. 13, pp. 38–54, Feb. 1994.

[17] M. Renaud and J. Y. Fourquet, "Minimum time motion of a mobile robot with two independent acceleration-driven wheels," in *Proc. IEEE Int. Conf. Robot. Autom.*, Apr. 1997, vol. 3, pp. 2608–2613.

[18] D. J. Balkcom and M. T. Mason, "Extremal trajectories for bounded velocity differential drive robots," in *Proc. IEEE Int. Conf. Robot. Autom.*, Apr. 2000, vol. 3, pp. 2479–2484.

[19] ——, "Time optimal trajectories for differential drive vehicles," *Int. J. Robot. Res.*, vol. 21, no. 3, pp. 199–217, Mar. 2002.

[20] H. Chitsaz, S. L. LaValle, D. J. Balkcom, and M. T. Mason, "Minimum wheel-rotation paths for differential-drive robots," in *Proc. IEEE Int. Conf. Robot. Autom.*, Apr. 2006, pp. 1616–1623.

[21] G. Kantor and A. A. Rizzi, "Feedback control of underactuated systems via sequential composition: Visually guided control of a unicycle," in *ISRR*, 2003, pp. 281–290.

[22] T. Ikeda, T. Mita, and B. D. O. Anderson, "Position and attitude control of an underwater vehicle using variable constraint control," in *Proc. IEEE Int. Conf. Decision, Control*, Dec. 2001, pp. 3758–3763.

[23] T. Ikeda, T. Nam, T. Mita, and B. D. O. Anderson, "Variable constraint control of underactuated free flying robots—Mechanical design and convergence," in *Proc. IEEE Int. Conf. Decision, Control*, Dec. 1999, pp. 2539–2544.

[24] E. J. Purcell, *Calculus with Analytic Geometry*. Englewood Cliffs, NJ: Prentice-Hall, 1978.

[25] S. Bhattacharya, "Optimal paths for landmark-based navigation by nonholonomic vehicles with field-of-view constraints," Master's thesis, Univ. Illinois at Urbana-Champaign, Urbana, IL, 2005.

Sourabh Bhattacharya received the B.Tech. degree in mechanical engineering in 2002 from the Indian Institute of Technology, Bombay, India, and the M.S. degree in electrical engineering in 2005 from the University of Illinois at Urbana-Champaign, where he is currently working toward the Ph.D. degree.

He is interested in control theory, motion planning, and computer vision. He has done work on optimal control of nonholonomic systems and is currently working on pursuit-evasion problems.

Rafael Murrieta-Cid (M'06) received the Ph.D. degree from the Institut National Polytechnique (INP), Toulouse, France, in 1998.

In 1998–1999, he was a Postdoctoral Researcher in the Computer Science Department, Stanford University, Stanford, CA. From September 2002 to July 2004, he was a Postdoctoral Researcher in the Beckman Institute, University of Illinois at Urbana-Champaign. From August 2004 to January 2006, he was a Professor and Director of the Mechatronics Research Center, Tec de Monterrey, Campus Estado de México, México. Since March 2006, he has been with the Mathematical Computing Group, Center for Mathematical Research, Guanajuato, México. He is mainly interested in sensor-based robot motion planning and computer vision.

Seth Hutchinson (SM'00–F'06) received the Ph.D. degree from Purdue University, West Lafayette, IN, in 1988.

In 1990, he joined the faculty of the University of Illinois at Urbana-Champaign, where he is currently a Professor with the Department of Electrical and Computer Engineering, the Coordinated Science Laboratory, and the Beckman Institute for Advanced Science and Technology. He has published more than 100 papers on the topics of robotics and computer vision, and is coauthor of *Principles of Robot Motion: Theory, Algorithms, and Implementations* (Cambridge, MA: MIT Press), and *Robot Modeling and Control* (New York: Wiley).

Dr. Hutchinson serves on the editorial boards of the *International Journal of Robotics Research* and the *Journal of Intelligent Service Robotics*. He served as Associate Editor and then Senior Editor for the IEEE TRANSACTIONS ON ROBOTICS AND AUTOMATION, now the IEEE TRANSACTIONS ON ROBOTICS, from 1997 to 2005. In 1996, he was a Guest Editor for a Special Section of the TRANSACTIONS devoted to the topic of visual servo control, and in 1994 he was Co-Chair of an IEEE Workshop on Visual Servoing. In 1996 and 1998, he coauthored papers that were finalists for the King-Sun Fu Memorial Best Transactions Paper Award. He was Co-Chair of the IEEE Robotics and Automation Society Technical Committee on Computer and Robot Vision from 1992 to 1996, and has served on the program committees for more than 50 conferences related to robotics and computer vision.